LANGMUIR
Article
pubs.acs.org/Langmuir

# Superior Water Sheeting Effect on Photocatalytic Titania Nanowire Coated Glass

Bálint Náfrádi,*[,†] Gábor Náfrádi,[‡] Carole Martin-Hamka,[†] László Forró,[†] and Endre Horváth*[,†]

[†]Laboratory of Physics of Complex Matter, Ecole Polytechnique Fédérale de Lausanne (EPFL), CH-1015 Lausanne, Switzerland
[‡]Institute of Nuclear Techniques (NTI), Budapest University of Technology and Economics (BME), H-1111 Budapest, Hungary

Supporting Information

**ABSTRACT:** Simple, rapid, and inexpensive fabrication of self-cleaning glass surfaces based on wet chemical deposition of $H_2Ti_3O_7$ (trititanate) and subsequent transformation of it into $TiO_2$ (anatase) nanowires on pristine glass surfaces is reported. Despite the low, 55%, surface coverage, the nanowire roughened glass surface showed self-cleaning properties comparable to much thicker, over 100-nm-thick, $TiO_2$ nanoparticle coated glasses. The superwettable surface showed 12° contact angle. Moreover, ultraviolet (UV) and natural light activated photocatalysis remained effective at enhancing the self-cleaning process in the case of the $TiO_2$ nanowire coated glass. Time-resolved study of the water droplet spread in millisecond time scales revealed that capillary forces induced by the random nanowire network significantly enhance the water sheeting effect of these textured glass surfaces. Time-resolved experiments revealed that the spreading velocity of the droplets were enhanced by 19% for the $TiO_2$ nanowire roughened surface and reached a $v_0$ = 508 mm/s initial spreading speed. Outdoor experiments validated the concept that $TiO_2$ nanowire coated glass possess self-cleaning properties with significantly reduced titania content compared to nanoparticle based films.

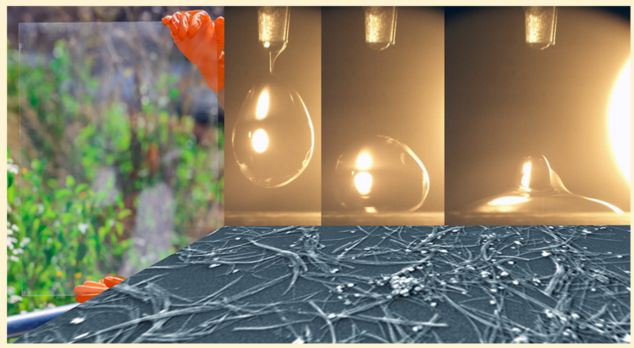

## 1. INTRODUCTION

Superwetting and antiwetting self-cleaning surfaces are in the forefront of applied research.[1−4] The general aim is to develop new materials and economically viable processes to create cheap, high quality, and durable self-cleaning coatings while minimally altering the optical properties of the underlying substrates. Functional materials possessing special wetting properties have an extensive range of applications, from antifogging and anti-icing surfaces, window glass cleaning, solar panel cleaning to water repellent cements and textiles.[5,6] Other potential market segments, where special wetting properties are highly desirable, are flexible or rigid displays, computer monitors, and smartphone screens, where, for example, fingerprints are undesirable. Similarly, photovoltaic panels, building and transport vehicle windows, could have multiple benefits from this technology. Advancements are expected by reducing performance loss due to dust accumulation, as well as the reduction of maintenance time and cost, lowering the environmental impact by reducing the use of detergents and water waste and finally by the elimination of tedious and sometimes dangerous (tall buildings and hard to reach areas) manual effort in cleaning work.

There are two major complementary categories to achieve self-cleaning surfaces: the hydrophilic and the hydrophobic strategies.[7] Hydrophobic self-cleaning surfaces are realized by the enhancement of the natural hydrophobicity of a surface, likewise increasing the water repellence.[8,9] These low adhesion, lotus-leaf-inspired surfaces[10] can be constructed by surface modifications with various chemicals and by creating a biomimetic, micro- and nanoscale surface topography.[3] As a result, on these antiwetting surfaces water droplets possess contact angle greater than 150°, meaning that on vertical or inclined surfaces dirt particles are picked up easily by nearly spherical water droplets and rolled away.[2,3]

A competing strategy to realize self-cleaning surfaces is to turn the surface hydrophilic.[1,5] In this case, the increased liquid adhesion induces enhanced spreading of water drops, i.e., the water sheeting effect rinses the dirt away. The technology has been successfully taken out from the laboratory environment to render ordinary glass surfaces into self-cleaning glass. Nowadays, the majority of commercially available self-cleaning glasses are based on a thin film titania ($TiO_2$) coatings.[11] These coatings clean the window in two stages, using two distinct properties: photocatalysis[12] and hydrophilicity. Due to the large (3−3.2 eV) bandgap of titania, photocatalytic decomposition of organic matter is activated under UV light ($\lambda$ < 400 nm); however, chemical modifications of titania allow tailoring the optical sensitivity by tuning the optical absorption.[13−16] When exposed to artificial light or natural sunlight, the reactive oxygen species (ROS) formed on the titania oxidize the organic

**Received:** May 29, 2017
**Revised:** July 21, 2017
**Published:** August 10, 2017




DOI: 10.1021/acs.langmuir.7b01790
*Langmuir* 2017, 33, 9043−9049

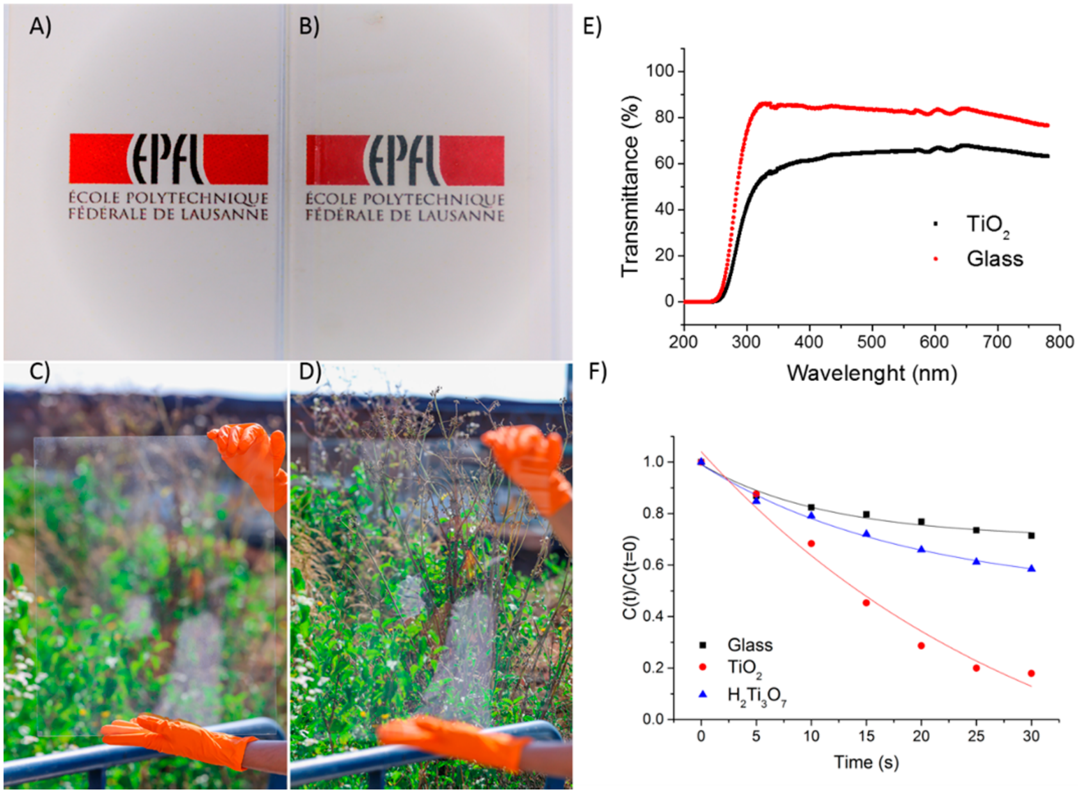


**Figure 1.** (A–D) Photographs of a 40 × 50 $cm^2$ glass sheet coated with $H_2Ti_3O_7$ nanowire demonstrating the excellent optical qualities of the self-cleaning glass. (A) and (B) Uncoated and $H_2Ti_3O_7$ nanowire coated glass, respectively. (C) Image focus is on the surface modified glass. (D) Image focus has been set behind the surface modified self-cleaning glass so as to demonstrate its optical transparency. (E) Optical transmittance of uncoated and coated glass by red and black, respectively. The transmittance in the visible spectral range dropped by less than 20% demonstrating that the functional self-cleaning surface maintains perfect optical quality. (F) Photocatalytic activity for uncoated glass, $TiO_2$ and $H_2Ti_3O_7$ coated surfaces. Lines are fit to an exponential decay model.

molecules adsorbed onto the surface.[4] Likewise, photocatalytic degradation of the organic molecules reduces the ability of inorganic dust particles to adhere to the surface. Additionally, surface hydrophilicity reduces contact angles of water droplets to lower values, causing the water to form a thin layer rather than droplets. Because of this water sheeting effect, the remaining inorganic dust particles will be washed away.[2,4]

Modifying the surface energy (wettability) of a given substrate is commonly achieved by controlling the roughness by micro- and nanostructuration.[9,17−24] Various techniques, including chemical vapor deposition, lithography, anodization, etching techniques (laser, plasma, chemical, and electrochemical) are available to create hierarchical nanosized geometrical features on a substrate.[9,17−24] Unlike these complex and multistep lithography patterning techniques, solution-based deposition processes require mild synthesis conditions and less energy. Therefore, thin film preparation by sol−gel methods[25] and nanoparticle deposition by spraying, blading, or printing considered as scalable and economically viable approaches to design patterned surfaces.[11]

Here, we report a facile surface patterning approach by liquid phase deposition of $H_2Ti_3O_7$ nanowires on glass surfaces and subsequent transformation of the $H_2Ti_3O_7$ nanowires to $TiO_2$ nanowires. We demonstrate photocatalytic activity and characterize both static and dynamic surface wettability. Experiments conducted under outdoor conditions verified the applicability of these titania nanowire roughened glass surfaces for various self-cleaning applications.[26]

## 2. EXPERIMENTAL METHODS

**2.1. Coating Preparation and Structural Preparation.** Titanate nanowires ($H_2Ti_3O_7$) have been prepared following the procedures reported in refs 13−16 and 27−30. Nanowire dispersion was prepared by adding 0.25 g $H_2Ti_3O_7$ nanowire in 100 mL of 2-propanol (>99.8% Merck), and the mixture is homogenized with an ultrasonic tip (Bandelin Sonopuls, Microtip MS73) at 10% amplitude for 30 min. Thin films were fabricated on microscopic glass substrates. The nanowire solution of 0.25 mg/mL in isopropyl alcohol is doctor bladed using a 40 $\mu$m spacer (3M) to obtain the desired surface coverage (∼50%). Once deposited onto glass slides the samples are heat treated at 150 °C in air for 2 h in order to evacuate the solvent.

Photocatalytic $TiO_2$ nanowires were prepared by a subsequent heat treatment of the $H_2Ti_3O_7$ nanowire coated glass sample at 400 °C in air. SEM characterization was performed with FEI/Philips XL30-FEG microscope with Electron Backscatter Diffraction analysis and Energy-Dispersive X-ray capability.

**2.2. Photocatalytic Test Reaction.** Photocatalytic test reactions were evaluated by methylene blue decomposition. A droplet of 3 $\mu$L of 50 mg/L methylene blue solution was deposited on each surface by a micropipette. Thirty minutes later the water evaporated and the absorbance value of the methylene blue spot was measured by UV−vis spectrophotometer (Carry 50 Scan). Next, the samples were placed in the spectrophotometer and illuminated by a mercury lamp (Hamamatsu LC5, 365 nm). The active surfaces were exposed to 1.2 mW, 365 nm UV light illumination for 30 min.

**2.3. Surface Wettability Measurements.** For static surface wettability measurements in ambient conditions 3 $\mu$L water droplet were pipetted to the surfaces. After 30 s, when the droplet reached equilibrium, a photograph was taken from the side and the contact angle was measured. The speed of evaporation and size of the droplet


DOI: 10.1021/acs.langmuir.7b01790
Langmuir 2017, 33, 9043−9049

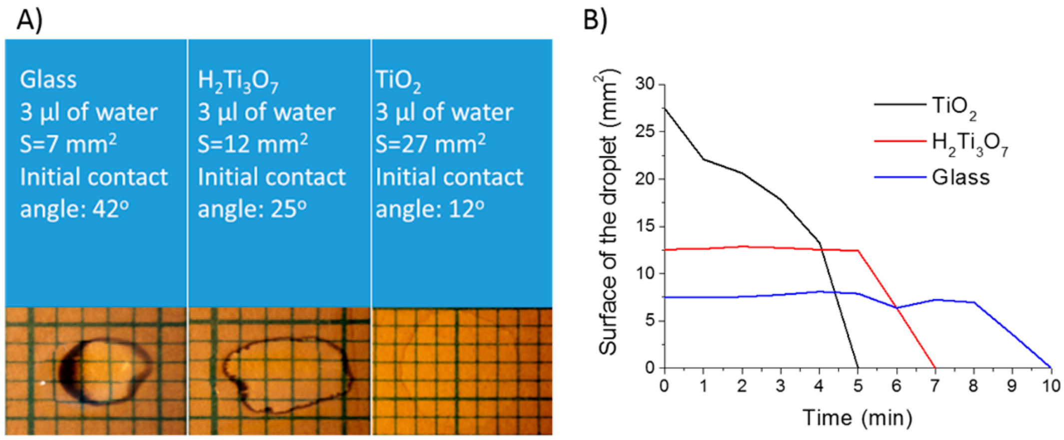


**Figure 2.** (A) Top view of the initial water droplets viewed from the top with the relevant parameters in the top. (B) Evolution of the surface as a function of time. Droplet with a larger initial surface evaporates faster.

was monitored from the top. For dynamic surface wettability measurements a Mikrotron MC 1363 fast camera was used.[31] The camera recorded, through an optical microscope, a side view of water drops hitting the different surfaces and then starting to spread away. For spatial scaling of the recorded images the end of the pipet was measured; the diameter of the pipet end was 0.72 mm. The obtained scale factor was 0.010778 mm/pixel. The size of the water drops was 15 $\mu$L. The drops were released from a few cm from above the surfaces, but as these surfaces act like mirrors[32] the impact velocity does not influence the spreading velocity. Two frame rates were used: 923 frame/s (fps) and 5490 fps.

**2.4. Outdoor Characterization.** Outdoor experiments under real environmental conditions were performed on the EPFL roof (GPS coordinates are 46.5191° N, 6.5668° E) in 2013. The samples were placed outdoors at an angle of 45° and kept outside for two months (April and May). In order to evaluate the effect of weathering on the optical properties, transmittance and SEM characterization were performed before and after two months of external weathering. Prior the SEM measurements the samples were coated with 5 nm of gold deposited by thermal evaporation.

## 3. RESULTS AND DISCUSSION

**3.1. Optical and Photocatalytic Properties.** A key property for self-cleaning glass applications is the high transparency of the applied coating in the visible spectral range. The titanate nanowire coatings were prepared from isopropyl alcohol solution by the doctor blading technique. The elongated titanate nanowires have a diameter of 30−100 nm and an average length of about 3 $\mu$m. Once deposited on the substrate they form an interconnected network, covering 55% of the surface, estimated from the analysis of the SEM images.[28] This solution-based patterning technique resulted in an about 20% transmittance loss as compared to the uncoated glass (Figure 1). The low transparency loss is similar to the case of $TiO_2$ nanoparticle coatings[11,33] and it does not impair optical use. The transparency loss remained low after transforming the $H_2Ti_3O_7$ NW coating to $TiO_2$ NW film by heat treatment (Figure 1e).

In order to evaluate the photocatalytic activity of the self-cleaning coatings, UV light-induced methylene blue discoloration test reactions were performed on the pristine, $H_2Ti_3O_7$ and $TiO_2$ nanowire coated glass. The rate constant was obtained by fitting an exponential decay model $C(t)/C(t = 0) = \exp(-t/\tau)$ to the data (lines in Figure 1f). The discoloration of methylene blue on the pristine glass corresponds to the direct photolysis under UV light with $\tau_{glass} = 94 \pm 13$ s. Importantly, the apparent reaction rates of methylene blue decomposition were around 5 times larger for the $TiO_2$ nanowire coated substrate as compared to the uncoated glass ($\tau_{TiO2} = 17 \pm 2$ s) (Figure 1f). This reflects the presence of photocatalytic activity of glass surface roughened with $TiO_2$ nanowires (Figure 1f). The methylene blue discoloration dynamics of our $TiO_2$ NW coatings are superior to $TiO_2$ film coatings ($\tau = 18-50$ s) and comparable to the standard Degussa P25 films ($\tau = 11-26$ s).[33]

**3.2. Static Surface Wetting Measurements.** Aside from the photocatalytic properties, the surface wettability is of paramount importance in self-cleaning application. In order to determine the surface philicity/phobicity, static wettability measurements were performed (Figure 2 and SI Figures 1 and 2). Water-droplet contact angles were determined from the side view of 3 $\mu$L droplets on a pristine glass, $H_2Ti_3O_7$ and $TiO_2$ nanowire coated glass (Figure 2 and SI Figure 2). A contact angle of 42° was measured on pristine glass. The simple solution based deposition of titanate nanowires lowered this value to 25°. In the case of the $TiO_2$ nanowire coated sample the static contact angle has further decreased to 12°. The contact angle for $TiO_2$ nanoparticle coatings decreasing by increasing coating thickness.[34] Similar water contact angle is observed for $TiO_2$ nanoparticle coatings thicker than 100 nm.[34] Remarkably, we reached this result by only 55% surface coverage of 10 nm average diameter $TiO_2$ NWs.

Top view photos allowed us to determine the surface area of the water droplets in contact with the substrate in equilibrium conditions (SI Figure 2). In ambient conditions, the 3 $\mu$L water droplet spread to a 4-times larger surface area on the titania nanowire surface modified glass as compared to the uncoated glass. Consequently, prevention of water beading accelerated the evaporation rate of water molecules. Droplets on the $TiO_2$ nanowire coated substrate dried twice as fast compared to the uncoated glass (Figure 2 and SI Figure 2). In practical application, this enhanced water sheeting and accelerated drying phenomena are essential to reduce the amount of unsightly streaks on a glass window. The formation of these spots are the consequence of the so-called coffee ring effect-type drying of water droplets containing dust particles.[35] From these static contact angle measurements we deduce that surface patterning (55% coverage) with titanium oxide nanowires has a strong influence on the equilibrium contact angle on the substrate.


DOI: 10.1021/acs.langmuir.7b01790
Langmuir 2017, 33, 9043−9049

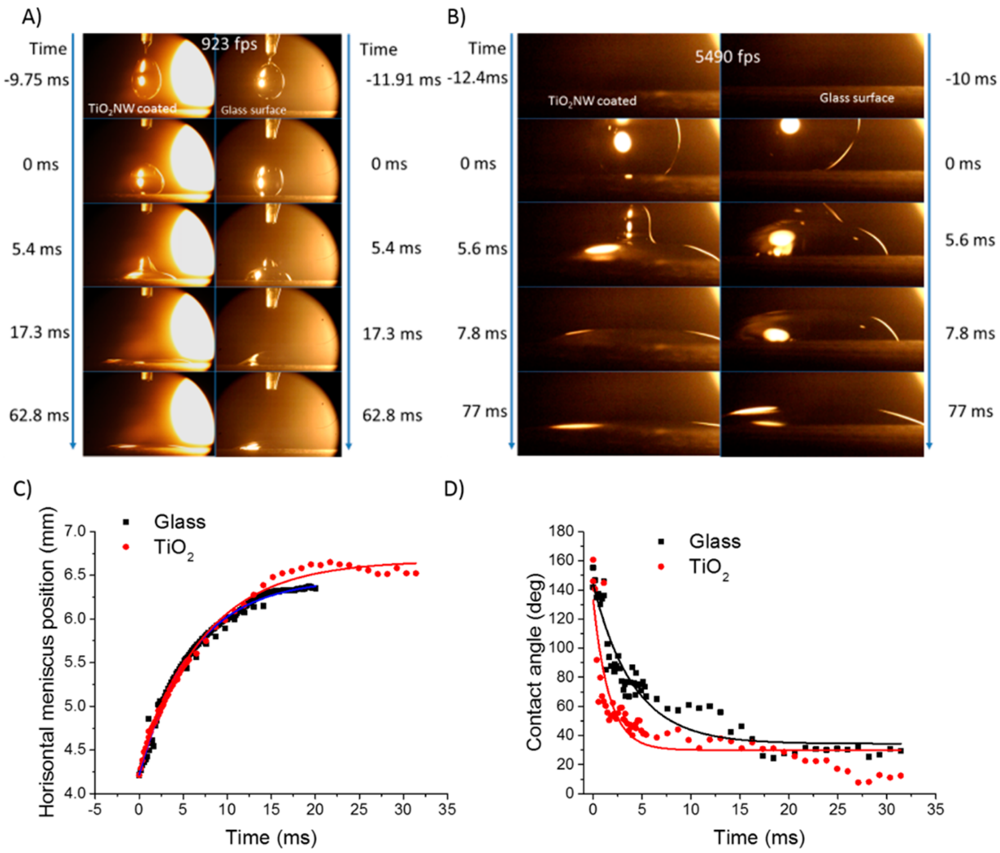


**Figure 3.** Time dependence of droplet formation and water sheeting with 923 and 5490 fps time resolution in panel (A) and (B), respectively. Left and right pictures are for $TiO_2$ nanowire coated and uncoated glass, respectively. Time-zero was set to the moment when the bottom of the droplet touches down to the surface. (C) The obtained meniscus positions during the spreading of the water drops as the function of time on the two examined surfaces (points). Simple saturation curves were fitted to both data set (lines for details see text). It is clearly visible that the meniscus of the water drop could reach ~75% larger distance from the impact position on the $TiO_2$ coated surface. (D) The measured contact angles during the drop spreading (points). Line is fit to an exponential model.

**3.3. Dynamic Surface Wetting Measurements.** In order to experimentally investigate the early stages of drop spreading dynamics we studied the sheeting effect on the millisecond time scale using a high speed camera. Here, the morphological behavior of an incoming rainwater droplet was simulated by pipetting a 15 $\mu$L distilled water droplet on the pristine and titania nanowire covered glass surfaces. Examples of the characteristic videos are show in Figure 3 with two different recording speeds of 923 and 5490 fps. The videos are also available as SI files. The first video (Figure 3a) gives an overview of the entire wetting process, while faster recording allows us to follow the initial surface wetting dynamics in greater detail (Figure 3b).

From the videos, the positions of the meniscuses, $A$, as a function of time, were obtained (Figure 3, SI files 2–5). An exponential saturation model, $A(t) = A^{\infty} - A^{0*} \exp(-t/\tau)$, was fit to the data in order to calculate the maximal spreading distance ($A^{\infty}$) from the impact positions. In agreement with the static measurements described in section 3.2, $A^{\infty}$ is larger for the $TiO_2$ nanowire coated surface, $\frac{A^{\infty}{}_{TiO_2}}{A^{\infty}{}_{Glass}} = 1.07 \pm 0.01$. We attribute this enhanced expansion to the enhancement of horizontal capillary forces due to the striped and elongated channels formed by $TiO_2$ nanowires on the surface.[35,36]

By numerically calculating the time derivative of the meniscus position the droplet speeding velocity is obtained. The spreading velocity of the droplets were enhanced by 19% for the $TiO_2$ nanowire roughened surface and reached a remarkable $v_0$ = 508 mm/s initial spreading speed. This enhanced velocity is also the natural consequence of the horizontal capillary forces acting on the meniscus.

The evolution of the contact angle as a function of time is shown on Figure 3c and d. In agreement with the droplet spread velocity observations, the contact angle decreases faster for the $TiO_2$ nanowire-textured glass compared to the untreated glass. Remarkably, it falls below 30° in less than 5 ms.

**3.4. Environmental Tests.** To validate the self-cleaning properties of $TiO_2$ nanotextured surfaces we performed environmental tests in real outdoor conditions. Optical transmittances before and after the external weather testing are compared in Figure 4 for the three different surfaces. The nontreated glass surface lost 40% of its original transmittance. The decrease in the transmittance is much lower on nanowire network covered glass. It is less than 5% in most of the studied 200–800 nm spectral range. This reflects significantly reduced dirt accumulation on nanowire-textured surfaces.

In principle, the decrease of the optical transmittance could be the consequence of two processes.[37] On one hand, structural degradation might lead to increased opacity.[37] On the other hand, contamination is caused by natural and anthropogenic air pollution: inorganic dust particles, carbon based particles from fuel and combustion, pollen, humic acid, bioactivity, etc.[38] SEM micrographs (Figure 5) unambiguously showed that the second mechanism, the accumulation of dirt on the surfaces from


DOI: 10.1021/acs.langmuir.7b01790
Langmuir 2017, 33, 9043–9049

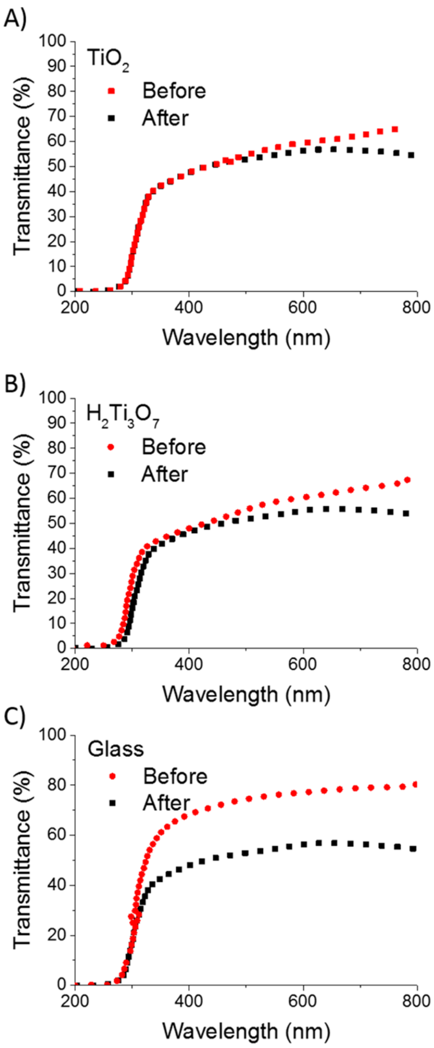


**Figure 4.** Comparison of the optical transmittance before and after the outdoor tests for the tree surfaces: $TiO_2$ nanowire coating, $H_2Ti_3O_7$ nanowire-textured glass, and uncoated glass in panels (A), (B), and (C), respectively. The optical degradation is clearly observable for the untreated glass (panel C).

chemical and biological sources, is responsible for the diminished optical transparency of the surfaces. SEM images showed that besides the inorganic particles, bacteria, fungi, and pollen were present on the nontreated glass surface (Figure 5a,c,e). The adhesion of organic material (pollen, humic acid) from the atmosphere serves as a glue and helps the accumulation of inorganic particles. With the rate depending on the climate and season, but on longer time scales (months), these processes will lead to a decreased transmittance of a glass. Unlike the pristine glass surface, the photocatalytic titania nanowire nanotextured glass showed the absence of bioactivity (Figure 5a,d,f). Only the presence of inorganic particles was confirmed by SEM imaging. We speculate that the biofilm formation was prevented as a result of two synergistic processes; natural sunlight induced photocatalysis and the capillary forces enhanced water sheeting effect under a rainfall.

### 3.5. Comparison to Other Self Cleaning Coatings.

There are many reports on photocatalytic $TiO_2$ based coatings in the literature which utilize sunlight and rinsing water to achieve self-cleaning functionality. Many trade-offs to balance the performance of the different coatings are also established.

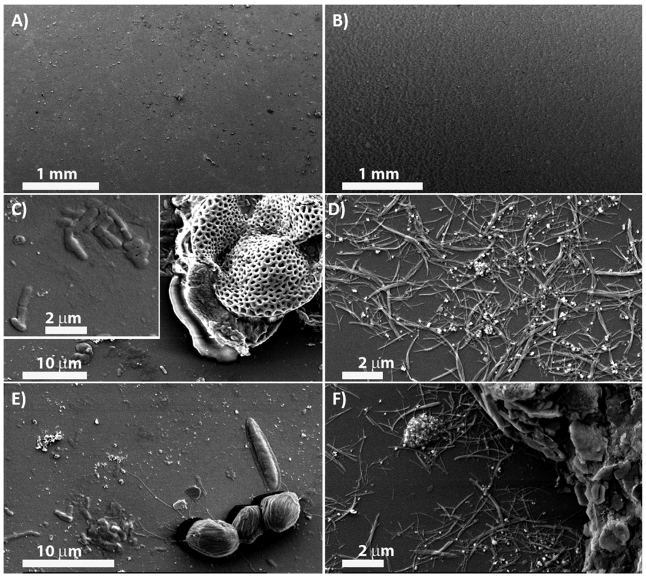


**Figure 5.** Representative SEM micrographs of the surfaces after the environmental tests in real outdoor conditions. (A), (C), (E) pristine glass. (B), (D), (F) $TiO_2$ nanowire coated glass. Bioactivity is observed in the untreated glass surface (A, C, E). In contrast, no biological pollution bioactivity was found on titania nanowire-textured glass surface (B, D, F).

The $TiO_2$ coating thickness should be minimized to reduce transparency loss and improve optical performance. In contrast, the $TiO_2$ coating thickness should be increased in order to decrease water contact angle and improve wettability. For $TiO_2$ particle based coatings in order to enhance photocatalytic activity a broad particle size distribution is preferable, while to maximize optical quality homogeneous particle size is desired. Accordingly, today self-cleaning glasses (e.g Pilkington Avtive, SGG BioClean, PPG SunClean) are commercially available and follow the above-mentioned trade-offs.

Here we show that another degree of freedom, the aspect ratio of the $TiO_2$ particles, can also be used to tailor these well-established trade-offs. In Table 1 we compare benchmarks like contact angle, transparency, and photocatalytic activity of various $TiO_2$ based self-cleaning glasses with our coating.The static contact angle and transparency is straightforward to compare. Photocatalytic activity, however, depends on the illumination conditions, which scatter across the literature. For that reason, we calculated relative photocatalytic activity compared to untreated glass of the same study as a baseline if data was available.

## 4. CONCLUSION

The low-cost, wet chemical deposition of semitransparent thin films composed of randomly oriented network of high aspect ratio photocatalytic titania nanowires is a scalable method of surface structuring glass surfaces with nanoscale stripes. The coatings are stable over 4 years. The coated glass surfaces, despite the low 55% coverage of the 30−100 nm thin $TiO_2$ NWs, demonstrate key self-cleaning properties: low, 12°, water contact angle and fast photodegradation of methylene blue ($\tau$ = 17 ± 2 s). Similar benchmarks are usually obtained for thick (over 100 nm) $TiO_2$ nanoparticle based films. These benign materials' properties we attribute the enlarged surface to volume ratio due to the nanowire morphology and to the capillary forces emerging from the nanosized channels defined


DOI: 10.1021/acs.langmuir.7b01790
Langmuir 2017, 33, 9043−9049

Table 1. Comparison of Key Parameters for Various Self-Cleaning Glasses

| sample | static contact angle (deg) | thickness (nm) | preparation method | transparency at 600 nm (%) | relative methylene blue decolorization for 1% photolysis (%) |
|---|---|---|---|---|---|
| Glass[a] | 42 | | | 92 | |
| $TiO_2$–NW[a] | 12 | 10[b] | | 74 | 3.98 |
| $H_2Ti_3O_7$ NW | 25 | 30–100[b] | | 74 | 1.52 |
| $TiO_2$[34] | 13 | 129 | electrospinning | 89 | |
| $TiO_2$[4] | 26–30 | 45.5 | Sol–gel | 90 | |
| $Si_{40}Ti_{60}$[4] | 1–6 | 63 | Sol–gel | 82 | |
| $Si_{86}Ti_{14}$[4] | 1–6 | 85 | Sol–gel | 85 | |
| $TiO_2$[26] | 66 | 300–400 | Sol–gel | 92 | 1.84 |
| $TiO_2$–Ag[26] | 48 | 3–4 | Liquid flame sprayed | 75 | 1.45 |
| Active[26] | 70 | 45 | chemical vapor deposition | 87.5 | 1.86 |

[a]The present study. [b]55% surface coverage.

by the nanowires. Ultrafast camera observations of the early stages of wetting confirmed that surface structuring with titania nanowire web reduces water contact angles to very low values and induces enhanced capillary force assisted wetting (water sheeting effect). Outdoor tests validated the concept that the enhanced water sheeting effect prevents water beading and enables rainwater to form a thin layer of continuous film taking the loosened microparticles with it instead of forming static droplets. Furthermore, another beneficial effect of water spread evenly on the nanowire coated glass surface is that the coated surface dries more quickly, leaving a reduced number of streaks and longer transparency in an outdoor application. Adhesion and long-term durability tests are needed to evaluate the stability of the titania nanowire web. We expect that self-cleaning glass applications will be facilitated by this economically viable surface structuring method.

## ■ ASSOCIATED CONTENT

### Supporting Information

The Supporting Information is available free of charge on the ACS Publications website at DOI: 10.1021/acs.langmuir.7b01790.

Wettability and contact angle measurements (PDF)
Video of Figure 3A (left) (AVI)
Video of Figure 3A (right) (AVI)
Video of Figure 3B (left) (AVI)
Video of Figure 3B (right) (AVI)

## ■ AUTHOR INFORMATION


### Corresponding Authors

*E-mail: nafradi@yahoo.com.
*E-mail: endre.horvath@epfl.ch.

### ORCID

Bálint Náfrádi: 0000-0001-9543-2970
Endre Horváth: 0000-0001-7562-2267


### Notes

The authors declare no competing financial interest.

## ■ ACKNOWLEDGMENTS

The work in Lausanne was supported by the Swiss National Science Foundation (Grant No. 200021_144419) and by grants from Switzerland through the Swiss Contribution (SH/7/2/20). Endre Horvath wants to thank the AIT grant, the Zeno-Karl Schindler foundation and MBR Global Water Initiatives for their support.

## ■ REFERENCES


(1) Ganesh, V. A.; Raut, H. K.; Nair, A. S.; Ramakrishna, S. A review on self-cleaning coatings. *J. Mater. Chem.* **2011**, *21* (41), 16304–16322.

(2) Nine, M. J.; Cole, M. A.; Johnson, L.; Tran, D. N. H.; Losic, D. Robust Superhydrophobic Graphene-Based Composite Coatings with Self-Cleaning and Corrosion Barrier Properties. *ACS Appl. Mater. Interfaces* **2015**, *7* (51), 28482–28493.

(3) Li, X.-M.; Reinhoudt, D.; Crego-Calama, M. What do we need for a superhydrophobic surface? A review on the recent progress in the preparation of superhydrophobic surfaces. *Chem. Soc. Rev.* **2007**, *36* (8), 1350–1368.

(4) Jesus, M. A. M. L. d.; Neto, J. T. d. S.; Timò, G.; Paiva, P. R. P.; Dantas, M. S. S.; Ferreira, A. d. M. Superhydrophilic self-cleaning surfaces based on TiO2 and TiO2/SiO2 composite films for photovoltaic module cover glass. *Applied Adhesion Science* **2015**, *3* (1), 5.

(5) Drelich, J.; Chibowski, E. Superhydrophilic and Superwetting Surfaces: Definition and Mechanisms of Control. *Langmuir* **2010**, *26* (24), 18621–18623.

(6) Li, S.; Huang, J.; Ge, M.; Cao, C.; Deng, S.; Zhang, S.; Chen, G.; Zhang, K.; Al-Deyab, S. S.; Lai, Y. Robust Flower-Like TiO2@Cotton Fabrics with Special Wettability for Effective Self-Cleaning and Versatile Oil/Water Separation. *Adv. Mater. Interfaces* **2015**, *2* (14), n/a.

(7) Adera, S.; Raj, R.; Enright, R.; Wang, E. N. Non-wetting droplets on hot superhydrophilic surfaces. *Nat. Commun.* **2013**, *4*, 1 DOI: 10.1038/ncomms3518.

(8) Sankar, S.; Nair, B. N.; Suzuki, T.; Anilkumar, G. M.; Padmanabhan, M.; Hareesh, U. N. S.; Warrier, K. G. Hydrophobic and Metallophobic Surfaces: Highly Stable Non-wetting Inorganic Surfaces Based on Lanthanum Phosphate Nanorods. *Sci. Rep.* **2016**, *6*, 22732.

(9) Han, J. T.; Xu; Cho, K. Diverse Access to Artificial Superhydrophobic Surfaces Using Block Copolymers. *Langmuir* **2005**, *21* (15), 6662–6665.

(10) Cheng, Y.-T.; Rodak, D. E. Is the lotus leaf superhydrophobic? *Appl. Phys. Lett.* **2005**, *86* (14), 144101.

(11) Paz, Y.; Luo, Z.; Rabenberg, L.; Heller, A. Photooxidative self-cleaning transparent titanium dioxide films on glass. *J. Mater. Res.* **1995**, *10* (11), 2842–2848.

(12) Fujishima, A.; Honda, K. Electrochemical Photolysis of Water at a Semiconductor Electrode. *Nature* **1972**, *238* (5358), 37–38.

(13) Szirmai, P.; Horváth, E.; Náfrádi, B.; Micković, Z.; Smajda, R.; Djokić, D. M.; Schenk, K.; Forró, L.; Magrez, A. Synthesis of Homogeneous Manganese-Doped Titanium Oxide Nanotubes from Titanate Precursors. *J. Phys. Chem. C* **2013**, *117* (1), 697–702.

(14) Jaćimović, J.; Horváth, E.; Náfrádi, B.; Gaál, R.; Nikseresht, N.; Berger, H.; Forró, L.; Magrez, A. From nanotubes to single crystals: Co doped $TiO_2$. *APL Mater.* **2013**, *1* (3), 032111.




DOI: 10.1021/acs.langmuir.7b01790
*Langmuir* 2017, 33, 9043–9049

(15) Szirmai, P.; Stevens, J.; Horváth, E.; Ćirić, L.; Kollár, M.; Forró, L.; Náfrádi, B. Competitive ion-exchange of manganese and gadolinium in titanate nanotubes. *Catal. Today* **2017**, *284*, 146−152.
(16) Szirmai, P.; Náfrádi, B.; Arakcheeva, A.; Szilágyi, E.; Gaál, R.; Nemes, N. M.; Berdat, X.; Spina, M.; Bernard, L.; Jaćimović, J.; Magrez, A.; Forró, L.; Horváth, E. Cyan titania nanowires: Spectroscopic study of the origin of the self-doping enhanced photocatalytic activity. *Catal. Today* **2017**, *284*, 52−58.
(17) Tadanaga, K.; Morinaga, J.; Matsuda, A.; Minami, T. Superhydrophobic−Superhydrophilic Micropatterning on Flowerlike Alumina Coating Film by the Sol−Gel Method. *Chem. Mater.* **2000**, *12* (3), 590−592.
(18) Kim, Y.; Lee, S.; Cho, H.; Park, B.; Kim, D.; Hwang, W. Robust Superhydrophilic/Hydrophobic Surface Based on Self-Aggregated Al2O3 Nanowires by Single-Step Anodization and Self-Assembly Method. *ACS Appl. Mater. Interfaces* **2012**, *4* (10), 5074−5078.
(19) Lee, S.; Kang, J. H.; Lee, S. J.; Hwang, W. Tens of centimeter-scale flexible superhydrophobic nanofiber structures through curing process. *Lab Chip* **2009**, *9* (15), 2234−2237.
(20) Marquez-Velasco, J.; Vlachopoulou, M.-E.; Tserepi, A.; Gogolides, E. Stable superhydrophobic surfaces induced by dual-scale topography on SU-8. *Microelectron. Eng.* **2010**, *87* (5−8), 782−785.
(21) Feng, J.; Tuominen, M. T.; Rothstein, J. P. Hierarchical Superhydrophobic Surfaces Fabricated by Dual-Scale Electron-Beam-Lithography with Well-Ordered Secondary Nanostructures. *Adv. Funct. Mater.* **2011**, *21* (19), 3715−3722.
(22) Kietzig, A.-M.; Hatzikiriakos, S. G.; Englezos, P. Patterned Superhydrophobic Metallic Surfaces. *Langmuir* **2009**, *25* (8), 4821−4827.
(23) Xu, L.; Karunakaran, R. G.; Guo, J.; Yang, S. Transparent, Superhydrophobic Surfaces from One-Step Spin Coating of Hydrophobic Nanoparticles. *ACS Appl. Mater. Interfaces* **2012**, *4* (2), 1118−1125.
(24) Ishizaki, T.; Hieda, J.; Saito, N.; Saito, N.; Takai, O. Corrosion resistance and chemical stability of super-hydrophobic film deposited on magnesium alloy AZ31 by microwave plasma-enhanced chemical vapor deposition. *Electrochim. Acta* **2010**, *55* (23), 7094−7101.
(25) Szabó, T.; Tóth, V.; Horváth, E.; Forró, L.; Szilagyi, I. Tuning the Aggregation of Titanate Nanowires in Aqueous Dispersions. *Langmuir* **2015**, *31* (1), 42−49.
(26) Piispanen, M.; Hupa, L. Comparison of self-cleaning properties of three titania coatings on float glass. *Appl. Surf. Sci.* **2011**, *258* (3), 1126−1131.
(27) Tétreault, N.; Horváth, E.; Moehl, T.; Brillet, J.; Smajda, R.; Bungener, S.; Cai, N.; Wang, P.; Zakeeruddin, S. M.; Forró, L.; Magrez, A.; Grätzel, M. High-Efficiency Solid-State Dye-Sensitized Solar Cells: Fast Charge Extraction through Self-Assembled 3D Fibrous Network of Crystalline $TiO_2$ Nanowires. *ACS Nano* **2010**, *4* (12), 7644−7650.
(28) Darányi, M.; Kukovecz, Á.; Horváth, E.; Kónya, Z.; Kiricsi, I. Fine tuning the coverage of a titanate nanowire layer on a glass substrate. *Chem. Phys. Lett.* **2008**, *460* (1−3), 191−195.
(29) Kukovecz, Á.; Hodos, M.; Horváth, E.; Radnóczi, G.; Kónya, Z.; Kiricsi, I. Oriented Crystal Growth Model Explains the Formation of Titania Nanotubes. *J. Phys. Chem. B* **2005**, *109* (38), 17781−17783.
(30) Horváth, E.; Kukovecz, Á.; Kónya, Z.; Kiricsi, I. Hydrothermal Conversion of Self-Assembled Titanate Nanotubes into Nanowires in a Revolving Autoclave. *Chem. Mater.* **2007**, *19* (4), 927−931.
(31) Mikrotron Mikrotron MC 1363 data sheet; ftp://ftp.stemmer-imaging.com/websites/documents/products/cameras/Mikrotron/en-Mikrotron-EoSens-high-speed-CMOS-camera-KMIK1-200903.pdf.
(32) Stapelbroek, B. B. J.; Jansen, H. P.; Kooij, E. S.; Snoeijer, J. H.; Eddi, A. Universal spreading of water drops on complex surfaces. *Soft Matter* **2014**, *10* (15), 2641−2648.
(33) Kenanakis, G.; Katsarakis, N. Chemically grown TiO2 on glass with superior photocatalytic properties. *J. Environ. Chem. Eng.* **2014**, *2* (3), 1748−1755.
(34) Ganesh, V. A.; Nair, A. S.; Raut, H. K.; Walsh, T. M.; Ramakrishna, S. Photocatalytic superhydrophilic TiO2 coating on glass by electrospinning. *RSC Adv.* **2012**, *2* (5), 2067−2072.
(35) Yunker, P. J.; Still, T.; Lohr, M. A.; Yodh, A. G. Suppression of the coffee-ring effect by shape-dependent capillary interactions. *Nature* **2011**, *476* (7360), 308−311.
(36) Khatavkar, V. V.; Anderson, P. D.; Meijer, H. E. H. Capillary spreading of a droplet in the partially wetting regime using a diffuse-interface model. *J. Fluid Mech.* **2007**, *572*, 367−387.
(37) Sutter, F.; Fernández-García, A.; Heller, P.; Anderson, K.; Wilson, G.; Schmücker, M.; Marvig, P. Durability Testing of Silvered-Glass Mirrors. *Energy Procedia* **2015**, *69*, 1568−1577.
(38) Yilbas, B. S.; Ali, H.; Khaled, M. M.; Al-Aqeeli, N.; Abu-Dheir, N.; Varanasi, K. K. Influence of dust and mud on the optical, chemical, and mechanical properties of a pv protective glass. *Sci. Rep.* **2015**, *5*, 15833.



DOI: 10.1021/acs.langmuir.7b01790
*Langmuir* 2017, 33, 9043−9049